Neuroscience Research 172 (2021) 80–86

Contents lists available at ScienceDirect

Neuroscience Research

journal homepage: www.elsevier.com/locate/neures

Protracted hypomobility in the absence of trigeminal sensitization after cortical spreading depolarization: Relevance to migraine postdrome

Mamoru Shibata[a,b,*,1], Satoshi Kitagawa[a], Chunghua Tang[a,c], Miyuki Unekawa[a], Yohei Kayama[a], Toshihiko Shimizu[a], Jin Nakahara[a], Norihiro Suzuki[a,d]

[a] Department of Neurology, Keio University School of Medicine, Tokyo, 160-8582, Japan
[b] Department of Neurology, Tokyo Dental College Ichikawa General Hospital, Chiba, 272-0513, Japan
[c] Department of Neurology and Centre for Clinical Neuroscience, Daping Hospital, Third Military Medical University, Chongqing, 400042, China
[d] Department of Neurology, Shonan Keiiku Hospital, Kanagawa, 252-0816, Japan

ARTICLE INFO

Article history:
Received 20 January 2021
Received in revised form 5 March 2021
Accepted 28 March 2021
Available online 2 April 2021

Keywords:
Migraine
Cortical spreading depolarization
Photophobia
Physical activity
Migraine postdrome
Neurotropin®

ABSTRACT

Migraine sufferers often exhibit photophobia and physical hypoactivity in the postdrome and interictal periods, for which no effective therapy currently exists. Cortical spreading depolarization (CSD) is a neural phenomenon underlying migraine aura. We previously reported that CSD induced trigeminal sensitization, photophobia, and hypomobility at 24 h in mice. Here, we examined the effects of CSD induction on light sensitivity and physical activity in mice at 48 h and 72 h. Trigeminal sensitization was absent at both time points. CSD-subjected mice exhibited significantly less ambulatory time in both light ($P = 0.0074$, the Bonferroni test) and dark ($P = 0.0354$, the Bonferroni test) zones than sham-operated mice at 72 h. CSD-subjected mice also exhibited a significantly shorter ambulatory distance in the light zone at 72 h than sham-operated mice ($P = 0.0151$, the Bonferroni test). Neurotropin® is used for the management of chronic pain disorders, mainly in Asian countries. The CSD-induced reductions in ambulatory time and distance in the light zone at 72 h were reversed by Neurotropin® at 0.27 NU/kg. Our experimental model seems to recapitulate migraine-associated clinical features observed in the postdrome and interictal periods. Moreover, Neurotropin® may be effective in ameliorating postdromal/interictal hypoactivity, especially in a light environment.

1. Introduction

Migraine is a debilitating chronic neurological disorder characterized by recurrent headache attacks accompanied by nausea/vomiting and heightened sensitivity to light and sound (Headache Classification Committee of the International Headache Society, 2018). A typical migraine headache is unilateral, pulsating, and aggravated by physical activity (Headache Classification Committee of the International Headache Society, 2018). Migraine, the second leading cause of years lived with disability (GBD 2016 Disease and Injury Incidence and Prevalence Collaborators., 2017), not only interferes with the daily lives of individuals, but also poses an enormous economic burden on society (Foster et al., 2020; Takeshima et al., 2019). Migraine has distinct phases, including premonitory, aura, headache, postdrome, and interictal (Dodick, 2018b). Although people with migraine suffer most during the headache phase, neurological symptoms are known to persist in the postdrome and interictal phases (de Tommaso et al., 2014; May, 2017). It has been shown that abnormal sensitivity to light (photophobia) and ocular allodynia are present in both ictal and interictal phases of migraine (Chu et al., 2011; McAdams et al., 2020; Mulleners et al., 2001; Perenboom et al., 2018). These symptoms can make working in a light environment more difficult. For instance, affected individuals may experience difficulty working on computer screens for a prolonged time, which is a considerable disadvantage given the contemporary work style. Moreover, recent data have demonstrated that patients with migraine have reduced physical activity on both non-headache days and headache days

Abbreviations: CI, Confidence intervals; CSD, Cortical spreading depolarization; FWHM, Full width at half maximum; NF-κB, Nuclear factor-kappa B.

* Corresponding author at: Department of Neurology, Keio University School of Medicine, 35 Shinanomachi, Shinjuku-ku, Tokyo, 160-8582, Japan.
E-mail addresses: mshibata@a7.keio.jp, mshibata@tdc.ac.jp (M. Shibata).
[1] Present address: Department of Neurology, Tokyo Dental College Ichikawa General Hospital, 5-11-13 Sugano, Ichikawa, Chiba 272-8513, Japan.

https://doi.org/10.1016/j.neures.2021.03.010

(Bond et al., 2015; Rogers et al., 2020). Asthenia, weakness, tiredness, and light sensitivity have been identified as major symptoms experienced during the migraine postdrome (Blau, 1982; Giffin et al., 2016; Kelman, 2006; Ng-Mak et al., 2011; Quintela et al., 2006).

The trigeminovascular system is thought to play a pivotal role in migraine pathogenesis (Ashina et al., 2019). Noseda et al. (2011) clarified that third-order trigeminovascular thalamic neurons send heavy projections to the motor and visual cortices, thus providing a neuroanatomical basis for the emergence of photophobia and hypoactivity in migraine. Cortical spreading depolarization (CSD), a neurophysiological correlate of migraine aura (Charles and Baca, 2013; Pietrobon and Moskowitz, 2014), is known to activate the trigeminovascular system (Iwashita et al., 2013; Zhang et al., 2011, 2010). We previously demonstrated that CSD caused trigeminal sensitization, photophobia, and hypoactivity in both light and dark zones at 24 h in mice, all of which were ameliorated by anti-migraine agents, sumatriptan and olcegepant (Tang et al., 2020). However, it remains unclear whether these symptoms persist beyond 24 h after CSD induction. If detected, prolonged abnormalities of trigeminal sensation, light sensitivity, and physical activity would provide a disease model for studying the mechanisms underlying postdrome and interictal phases of migraine. Our behavioral assay allows us to explore the effect of CSD on mobility beyond 24 h.

Neurotropin® is a non-protein fraction extracted from the inflamed skin of rabbits after inoculation with vaccinia virus, and has been traditionally used for the treatment of various chronic pain conditions, mainly in Asian countries. Clinical evidence for the efficacy of Neurotropin® in alleviating headache disorder is scarce, although it has been reported that treatment with Neurotropin® relieved nummular headache (Danno et al., 2013). Given that Neurotropin® contains a multitude of bioactive substances, it exerts various actions, ranging from neurotrophic effects (Fukuda et al., 2010, 2015; Nakajo et al., 2015) to inflammatory modulation (Fukuda et al., 2020; Kato et al., 1991; Nishimoto et al., 2016; Yoshii et al., 1987). Numerous complex pathways are thought to be involved in the analgesic effect of Neurotropin®.

In the present study, we examined CSD-induced changes in trigeminal sensation and physical activity at 48 and 72 h. We also explored the effect of Neurotropin® administration on CSD-induced physical activity.

2. Materials and methods

2.1. Animals

The present study was approved by the Laboratory Animal Care and Use Committee of Keio University (approval no. 14,084). Male C57BL/6 mice aged 8–12 weeks were obtained from CLEA Japan Inc. (Fujinomiya, Japan). A total of 55 mice were used in the present study. They were kept in an ambient specific-pathogen-free condition with a 12-h light/dark cycle and had free access to food and water. All experiments were performed in accordance with the National Institute of Health Guide for the Care and Use of Laboratory Animals (NIH Publications No. 80-23) revised in 1996.

2.2. Drug administration

Neurotropin® solution (20 NU/mL; Nippon Zoki Pharmaceutical Co., Ltd., Osaka, Japan) was dissolved in normal saline. Neurotropin® was slowly administered at 0.27 NU/kg or 0.81 NU/kg in 200 μL solution using a feeding needle (18060−20, Fine Science Tools, Foster City, USA). These doses are comparable to those used for treating neuropathic pain. The same volume of normal saline was administered as a vehicle. Drug administration was carried out 30 min before CSD induction. There were four different experimental groups in the present study, as follows: the Sham-Vehicle group, the CSD-Vehicle group, the CSD-NT 0.27 (Neurotropin® 0.27 NU/kg) group, and the CSD-NT 0.81 (Neurotropin® 0.81 NU/kg) group.

2.3. CSD induction

Under isoflurane anesthesia (1–2%), the mouse head was fixed in a stereotaxic apparatus. Non-invasive monitoring of systolic blood pressure and heart rate was performed using a non-invasive blood pressure monitor (MK-2000ST; Muromachi Kikai Co., Ltd., Tokyo, Japan). Body temperature was kept at around 37 °C using a thermistor-regulated heating pad (BWT-100; Bioresearch Center Co., Ltd., Nagoya, Japan).

For electrophysiological recordings, three burr-holes were drilled into the left part of the skull. The posterior hole at the coordinates of 5 mm posterior and 2 mm lateral to the bregma was used for KCl administration. The parietal hole (2 mm lateral and 2 mm caudal to the bregma) and the frontal hole (2 mm lateral and 2 mm rostral to the bregma) were drilled to install the recording electrodes. Two Ag/AgCl DC electrodes (tip diameter =200 μm, EEG-5002Ag; Bioresearch Center Co., Ltd.) were installed on the dura at the parietal (proximal) and frontal (distal) holes. A DC potential was applied at 1–100 Hz and digitized at 1 kHz using an extracellular amplifier (Model 4002 and EX1; Dagan Co., Minneapolis, MN, USA). Continuous recordings of the DC potential were stored on a multi-channel recorder (PowerLab 8/30; ADInstruments, Ltd., Sydney, Australia). After confirming that all parameters were stable for at least 10 min, CSD was induced by applying KCl solution (1.0 mol/L, 5 μL) onto the dura. The induction of CSD was verified by the appearance of a distinct DC potential deflection. CSD was induced five times after washing the cortical surface with normal saline. After the surgery, all electrodes were removed, and the craniotomies were closed. In sham-operated mice, all surgical procedures were performed except for the chemical stimulation with KCl solution and DC electrode insertion. Sham-treated mice and CSD-subjected mice were anesthetized for equivalent periods of time. In the present paper, we refer to the CSD operation and sham operation collectively as surgery.

The CSD propagation velocity and full width at half maximum (FWHM) were measured. The CSD propagation velocity was calculated on the basis of the latency and distance between the proximal and distal electrodes. The FWHM was determined from the curves recorded at the distal electrode.

2.4. Facial heat pain threshold temperature measurement

The detailed protocol for heat pain threshold temperature has been described elsewhere (Kayama et al., 2018). Briefly, after acclimation to the experimental apparatus and facial hair removal, a pair of Peltier module bars with a surface temperature regulated between 36 °C and 56 °C was applied bilaterally to the lateral aspect of the face. The bar surface temperature was gradually elevated from 36 °C by 1 °C/4 s until face withdrawal. Mouse behaviors were monitored using a video recorder (Panasonic, Kadoma, Japan). Videos were analyzed by an examiner who was blinded to group allocation of the animals. The lowest temperature at which a mouse turned its head away from the heating bars was considered as the heat pain threshold temperature. In each session, the threshold temperature was measured five times. The measurement was carried out before surgery and 48 h and 72 h after surgery.

In our preliminary experiments, the standard deviation of the heat pain threshold temperature of normal mice was found to be 0.8–1.0 °C. When the type I error rate and power were 5% and 0.80,

respectively, the sample size required to detect a 0.5 °C difference was calculated as 40–60 trials in each group.

2.5. Mouse locomotion assay in the light and dark zones

The detailed protocol for this assay has been described elsewhere (Tang et al., 2020). Briefly, mouse behavior was continuously recorded in a testing chamber (27 cm wide × 27 cm deep × 20.3 cm high) with three sets of 16-beam infrared arrays (two sets of perpendicular beams crossed at a height of 1.0 cm to detect mouse location and locomotion, and the third beam crossed the width of the chamber at a height of 7.3 cm to detect vertical activity; Med Associates, Fairfax, VT). The testing field was equally divided into light and dark zones using a dark insert (Med Associates). The mice were allowed to move between the two zones through an opening (5.2 cm × 6.8 cm). The light intensity measured at a height of 2 cm in the light zone was 540 lx, whereas the intensities measured in the dark zone were 380 lx immediately inside the orifice, 20 lx at the center, and 5 lx at the corners. Mouse activity was analyzed using a computer equipped with Activity Monitor v6.02 (Med Associates).

Mice were allowed to acclimatize to the test chamber, as described previously (Tang et al., 2020). The acclimation was carried out prior to the surgery. At 48 and 72 h after the CSD or sham operation, locomotor activity was recorded for 30 min with the lights on. The total time spent in the light field was used to evaluate light aversion. For all mice examined, behavioral testing was carried out between 10:00 and 18:00 in a quiet room.

2.6. Assessment of mouse locomotor activity

The effects of Neurotropin® administration on mouse locomotion in both compartments were evaluated using several movement parameters. When mice moved out of the 6.35 cm × 6.35 cm square box around them within 0.5 s, their movements were defined as ambulatory. Ambulatory distance (cm) was defined as the total distance travelled during ambulatory movement. Ambulatory average velocity (cm/s) was calculated as the ambulatory distance divided by ambulatory time, which was defined as the time spent in the ambulatory movement status. Our preliminary experiments revealed that the standard deviation of the total time spent in the light zone of untreated control mice was 120–150 s. With a type I error rate and power of 5% and 0.80, respectively, the sample size required to detect a 200 s difference was calculated as 6–9 subjects in each group.

2.7. Statistical analyses

Numerical data relevant to physiological and CSD-related electrophysiological parameters are expressed as the mean ± SD. The heat pain threshold temperatures and locomotion data are shown using 95 % confidence intervals (CIs). Between-group comparisons of physiological parameters and CSD-related electrophysiological data were made using the Kruskal–Wallis test. A two-way repeated-measures ANOVA was used to evaluate the effects of CSD induction and pharmacological interventions on the temporal trajectories of the heat pain threshold temperature, total time spent in the light zone, ambulatory time, and distance travelled in each zone. Post-hoc multiple comparisons were carried out using the Bonferroni test. Mean differences are indicated by 95 % CI. Data were analyzed using GraphPad Prism 8 software (GraphPad Software, San Diego, CA).

Table 1
CSD-related electrophysiological parameters.

	CSD-Vehicle	CSD-NT 0.27	CSD-NT 0.81	P-value
Number of animals	8	8	8	
Propagation velocity (mm/min)	4.2 ± 0.6	5.0 ± 1.1	4.2 ± 0.6	0.3901
FWHM (s)	41.3 ± 3.3	42.8 ± 10.1	45.8 ± 2.9	0.4825

3. Results

3.1. Physiological parameters, body weight, and CSD-related electrophysiological parameters

The timeline of the present study is shown in Fig. 1A. Craniotomies for CSD induction and installation of electrodes and experimental probes are shown in Fig. 1B. A representative recording of CSD induction is illustrated in Fig. 1C, with concrete measurements for CSD propagation velocity (Fig. 1D) and FWHM (Fig. 1E). We observed no significant between-group differences in systolic blood pressure, heart rate, or body weight (data not shown). There was no significant effect of Neurotropin® administration on CSD-related electrophysiological parameters (propagation velocity and FWHM; Table 1).

3.2. Effects of CSD on facial heat pain threshold temperature at 48 h and 72 h after CSD induction

A two-way ANOVA showed that there was no significant effect of time or CSD induction on the facial heat pain threshold temperature at 48 and 72 h after surgery (time: $F_{(2,228)}$ = 1.011, P = 0.3655; CSD induction: $F_{(1,114)}$ = 0.05389, P = 0.8168). The mean differences of facial heat pain threshold vs. the baseline value were -0.21 °C (95 % CI: -0.74–0.32, P > 0.9999) and -0.02 °C (95 % CI: -0.56–0.51, P > 0.9999) at 48 h and 72 h, respectively.

3.3. Effects of CSD induction and Neurotropin® pretreatment on the total time spent in the light zone

We explored the effects of CSD induction and Neurotropin® administration on the total time spent in the light zone at 48 h and 72 h after surgery. A two-way ANOVA did not detect a main effect of observation time on the time spent in the light zone (P = 0.1486). While the effect of CSD induction and Neurotropin® administration did not reach significance ($F_{(1,28)}$ = 2.207, P = 0.0787), there was a trend towards a shorter total time spent in the light zone in the CSD-Vehicle group as compared with the Sham-Vehicle group at 72 h (mean difference: −327 s [95 % CI: -672.3–18.32], P = 0.0732, the Bonferroni test). Moreover, Neurotropin® (0.27 NU/kg) tended to reverse the CSD-induced decrease on the time spent in the light zone (mean difference: 343.4 s [95 % CI: -1.941–688.7], P = 0.0521, the Bonferroni test).

3.4. Effects of CSD and Neurotropin® pretreatment on ambulatory time in the light and dark zones

We then analyzed the effects of CSD alone and combined with Neurotropin® pretreatment on ambulatory time in the light and dark zones separately at 48 h and 72 h after surgery. In the light zone, a two-way ANOVA detected a significant main effect of CSD induction and Neurotropin® administration ($F_{(3,28)}$ = 5.254, P = 0.0053), while there was no significant main effect of observation time ($F_{(1,28)}$ = 0.372, P = 0.5468) (Fig. 2A). There was a significant difference in ambulatory time in the light zone between the Sham-Vehicle group and the CSD-Vehicle group (mean difference: -26.07

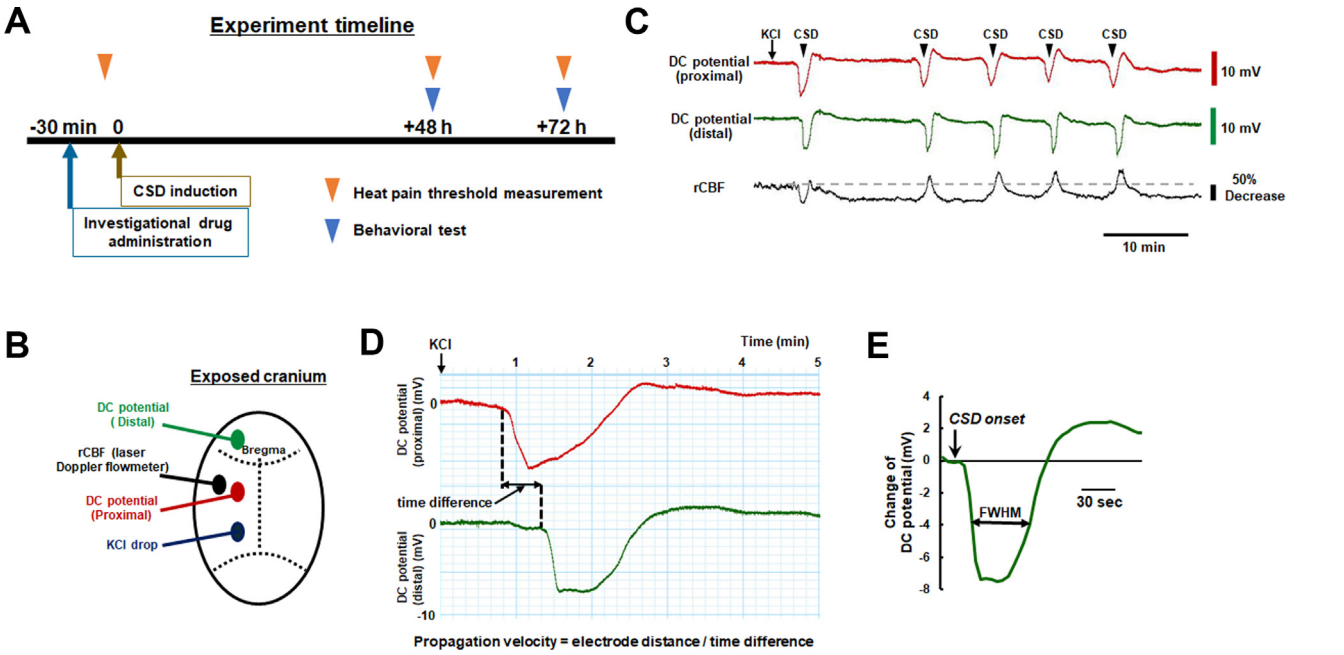

Fig. 1. Experiment timeline and measurements for CSD-related electrophysiological parameters. (A) Experimental timeline for the measurement of facial heat pain threshold temperature and the light/dark box behavioral test. Facial heat pain threshold measurements were performed immediately before and 48 and 72 h after CSD induction (orange triangles). The light/dark box behavioral testing was performed at 48 and 72 h after CSD induction (green triangles). Investigational drugs, including the vehicle, were administered 30 min prior to CSD induction.
(B) Craniotomies for CSD induction and installation of experimental probes. (C) A representative recording of CSD induction. (D) Measurement of CSD propagation velocity. (E) Measurement of FWHM.

s [95 % CI: -47.03–-5.109], P = 0.0074, the Bonferroni test) and between the CSD-Vehicle group and the CSD-NT 0.27 group (mean difference: 29.65 s [95 % CI: 8.69–50.61], P = 0.0017, the Bonferroni test) at 72 h (Fig. 2A). A two-way ANOVA did not detect a significant main effect of time in the dark zone ($F_{(1,28)}$ = 0.09536, P = 0.7598), while the effect of CSD induction with Neurotropin® administration on ambulatory time in the dark zone nearly reached significance ($F_{(3,28)}$ = 2.717, P = 0.0636) (Fig. 2A). There was a significant difference in ambulatory time in the dark zone between the Sham-Vehicle group and the CSD-Vehicle group only (mean difference: -22.55 s [95 % CI: -44.09–-1.007], P = 0.0354, the Bonferroni test) at 72 h (Fig. 2A).

3.5. *Effects of CSD and Neurotropin® pretreatment on ambulatory distance in the light and dark zones*

We also examined the effects of CSD alone and combined with Neurotropin® administration on ambulatory distance in the light and dark zones at 48 h and 72 h after surgery. In the light zone, a two-way ANOVA revealed a significant main effect of CSD induction and Neurotropin® administration on ambulatory distance ($F_{(3,28)}$ = 5.138, P = 0.0059), while there was no significant main effect of observation time ($F_{(1,28)}$ = 0.3289, P = 0.5709) (Fig. 2B). There was a significant difference in ambulatory distance in the light zone between the Sham-Vehicle group and the CSD-Vehicle group (mean difference: -933.5 cm [95 % CI: -1741–126.2], P = 0.0151, the Bonferroni test) and between the CSD-Vehicle group and the CSD-NT 0.27 group (mean difference: 1142 cm [95 % CI: 335.1–1950], P = 0.0017, the Bonferroni test) at 72 h (Fig. 2B).

In the dark zone, a two-way ANOVA did not detect any significant main effects of observation time ($F_{(1,28)}$ = 0.4041, P = 0.5301) or CSD induction and Neurotropin® pretreatment ($F_{(3,28)}$ = 2.469, P = 0.0827) on ambulatory distance (Fig. 2B). The CSD-NT 0.27 group tended to exhibit a greater ambulatory distance than the CSD-Vehicle group (mean difference: 750.7 cm [95 % CI: -5.714–1507], P = 0.0528, the Bonferroni test) at 72 h (Fig. 2B).

3.6. *Between-group comparison of average ambulatory speed*

The average ambulatory speed was unaltered by CSD. Furthermore, treatment with Neurotropin® at either dose did not affect the average ambulatory speed (Fig. 2C).

4. Discussion

Untreated migraine attacks may persist for up to 72 h (2018), which is why we examined trigeminal sensitization and physical activity at 48 h and 72 h after CSD in the present study. The most notable finding was that CSD deteriorated hypomotility in the light and dark zones, even after trigeminal sensitization had worn off. It is unlikely that this reduced locomotor activity resulted from muscle weakness and motor paralysis, because the average ambulatory speed was unaffected by CSD. We previously reported that the same CSD insult as that used in the present study caused trigeminal sensitization, photophobia, and hypomotility at 24 h as compared with sham-operated mice (Tang et al., 2020). However, the present study revealed that there were no between-group differences at 48 h in any of these parameters. At 72 h, mouse ambulatory time exhibited a tendency to recover compared to that seen at 48 h in the sham-operated mice, whereas the ambulatory time of CSD-affected mice continued to deteriorate. Overall, CSD-induced hypomobility exhibited a diphasic change. Such prolonged hypomotility was more evident in the light zone, as evidenced by significant reductions in both ambulatory time and ambulatory distance. Concomitantly, the CSD-affected mice tended to spend less time in the light zone than sham-operated mice. Hence, it is suggested that light aversion may play a role in the hypomotility. Our previous data demonstrated that trigeminal thermal allodynia was present at 24 h in an identical CSD model (Tang et al.,

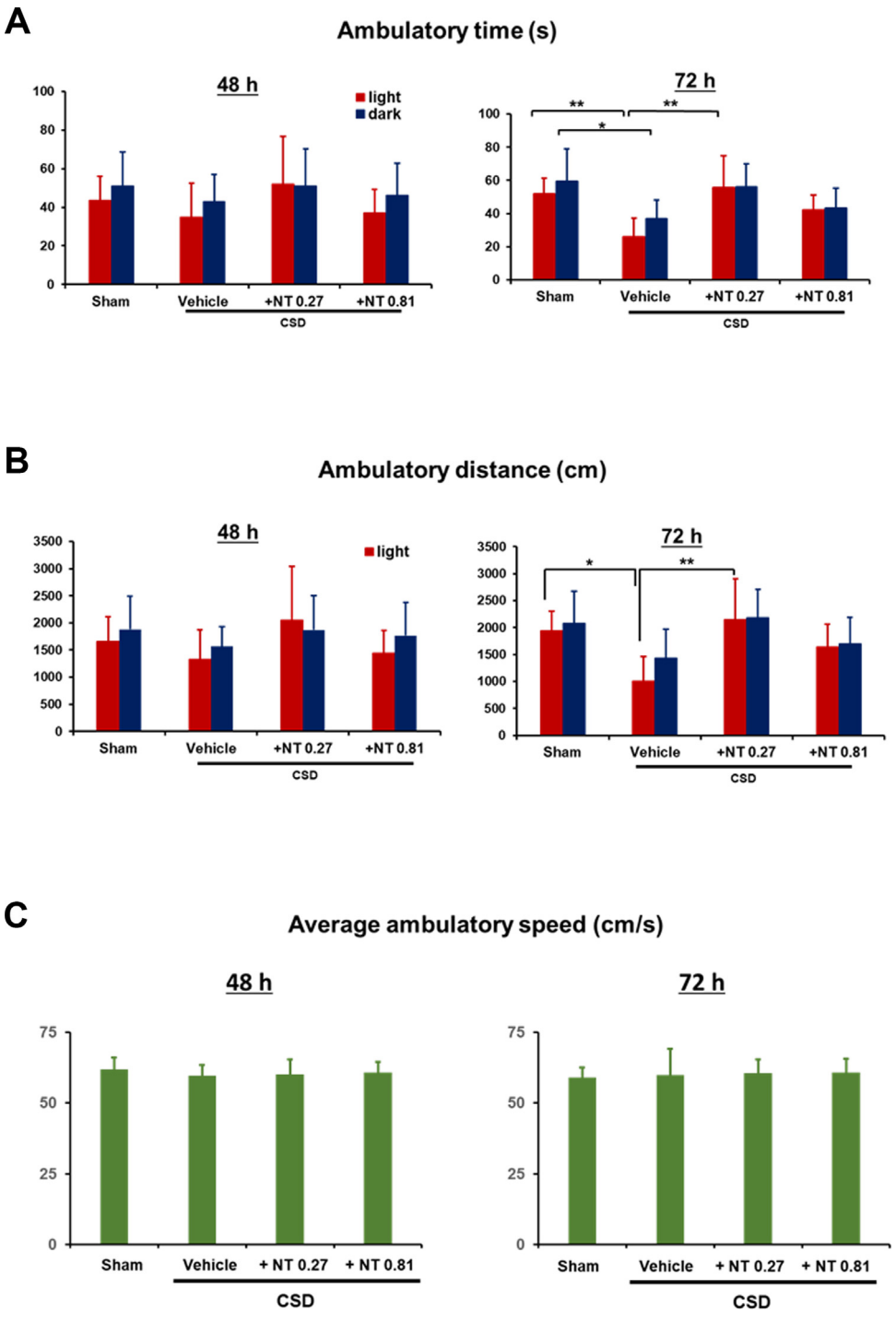

Fig. 2. (A) Ambulatory time in the light and dark zones in each group. The graphs show the ambulatory time (s). Red and blue bars indicate light and dark data, respectively. The data are presented as mean ± SD. A two-way repeated-measures ANOVA was used to evaluate the effects of CSD induction, Neurotropin® pretreatment, and observation time. Multiple comparisons were performed using the Bonferroni test (*P < 0.05, **P < 0.01). N = 8 in each group.
(B) Ambulatory distance in the light and dark zones in each group. The graphs show the ambulatory distance (cm). Red and blue bars indicate light and dark data, respectively. The data are presented as mean ± SD. A two-way repeated-measures ANOVA was used to evaluate the effects of CSD induction, Neurotropin® pretreatment, and observation time. Multiple comparisons were performed using the Bonferroni test (*P < 0.05, **P < 0.01). N = 8 in each group.
(C) Average ambulatory speed in each group. The graphs show the average ambulatory speed (cm/s). The data are presented as mean ± SD. A two-way repeated-measures ANOVA was used to evaluate the effects of CSD induction, Neurotropin® pretreatment, and observation time. Multiple comparisons were performed using the Bonferroni test. N = 8 in each group.

2020). Consistently, a previous *in vivo* study using intravital recording of electrical activity of the dura-innervating trigeminal ganglion neurons showed that CSD caused mechanical sensitization (Zhang et al., 2010). Furthermore, the firing rate of neurons receiving dural nociceptive signals in the trigeminal nucleus caudalis was elevated by CSD (Zhang et al., 2011). These *in vivo* studies did not present any data on trigeminal sensitization beyond 120 min after CSD induction. The present results indicate that CSD-induced trigeminal sensitization wears off by 48 h. Importantly, we demonstrated that avoidance of headache-worsening factors (light and physical

activity) extends beyond the period of trigeminal sensitization after CSD. This could indicate that the CSD-affected mice in our study were conditioned to associate light exposure and physical activity with pain, rather than to avoid moving because of actual pain. The salience network plays a key role in the evaluation of the state or condition of a threat to an organism (Borsook et al., 2013). It has been reported that the function of the salience network is altered in actual migraine sufferers (Maleki et al., 2012) and an inflammatory soup-based rat migraine model (Becerra et al., 2017). Our findings could therefore be explained by dysfunction of the salience network.

The time points selected for the present study (48 h and 72 h after CSD induction) may capture the condition that is analogous to the postdromal phase of migraine. Photophobia, tiredness, and weakness are frequently observed in the postdrome of migraine (Blau, 1982; Giffin et al., 2016; Kelman, 2006; Ng-Mak et al., 2011; Quintela et al., 2006); tiredness and weakness can reduce physical activity, and most patients find postdrome symptoms debilitating (Blau, 1982; Giffin et al., 2016; Kelman, 2006; Ng-Mak et al., 2011; Quintela et al., 2006). Photophobia and hypoactivity impair quality of life and lead to reduced productivity at work. In particular, photophobia is likely to interfere with work that requires the use of a computer screen (Chu et al., 2011; McAdams et al., 2020; Mulleners et al., 2001; Perenboom et al., 2018). Currently, there is no established therapy for these symptoms. Our data demonstrated that pretreatment with Neurotropin® at 0.27 NU/kg reversed CSD-induced decreases in ambulatory time and distance in the light zone. A dose of 0.27 NU/kg is used for treating neuropathic pain in humans (Hata et al., 1988). Thus, the optimal therapeutic dose of Neurotropin® for neuropathic pain may be effective for migraine-associated photophobia and hypoactivity postdrome. Our findings can be clinically translated into situations in which Neurotropin® pretreatment can ameliorate hypoactivity in a light environment in the postdrome period, thus allowing patients to regain functionality and productivity. It remains unknown how Neurotropin® improved photophobia and hypoactivity in our migraine model. The biological actions of Neurotropin® include suppression of proinflammatory cytokine production (Fukuda et al., 2020; Nishimoto et al., 2016), enhanced serotonin and noradrenergic activity (Okazaki et al., 2008), glycosaminoglycan synthesis (Sakai et al., 2018), and inhibition of nuclear factor-kappa B (NF-κB) and mitogen-activated protein kinase signaling pathways (Zheng et al., 2018). Intriguingly, a recent study reported the involvement of NF-κB and NF-E2-related factor 2 pathway-mediated neuroinflammation in nitroglycerin-induced migraine-like symptoms and photophobia (Casili et al., 2020). As mentioned above, migraine sufferers often complain of photophobia and reduced physical activity throughout the interictal period (Bond et al., 2015; Chu et al., 2011; McAdams et al., 2020; Mulleners et al., 2001; Perenboom et al., 2018; Rogers et al., 2020). It would be worth exploring whether chronic administration of Neurotropin® improves these disabling conditions.

The present study has several limitations that should be noted. First, the CSD-based migraine model mimics migraine with aura attacks, and so it remains unclear whether our findings are also applicable to migraine without aura. Second, the invasive nature of the disease model means that comparisons relevant to physical activity were only made between CSD-subjected mice and sham-operated mice at identical timepoints in the present study. As described in the materials and methods section, electrode insertion into the brain tissue was not done in the sham surgery, because we observed that electrode insertion could induce CSD incidentally. Third, migraine is approximately three times more prevalent in women that in men (Dodick, 2018a). Nevertheless, we only used male mice to exclude the potential effects of menstruation on behavior (Ebine et al., 2016). A recent paper reported that there is no significant sex difference in CSD-induced behavioral patterns (Harriott et al., 2021). Finally, as stated above, we did not elucidate the mechanism by which Neurotropin® ameliorated physical activity in CSD-affected mice, which should be clarified in future studies.

In summary, our experimental model provides a platform from which to further investigate postdromal photophobia and hypoactivity in migraine. Our findings offer a novel direction for future migraine research. Furthermore, Neurotropin® may confer protection against these unrecognized and undertreated symptoms at a dose used for the management of neuropathic pain in clinical settings.

Author contributions

Mamoru Shibata: Conceptualization, Methodology, Format analysis, Investigation, Writing-Original Draft, Supervision, Fund acquisition.
Satoshi Kitagawa: Investigation, Writing - Review & Editing.
Chunghua Tang: Methodology, Format analysis, Investigation, Writing - Review & Editing, Fund Acquisition.
Miyuki Unekawa: Investigation, Writing - Review & Editing.
Yohei Kayama: Investigation, Writing - Review & Editing.
Jin Nakahara: Writing - Review & Editing.
Norihiro Suzuki: Writing - Review & Editing, Fund Acquisition.

Funding

This study was supported by JSPS KAKENHI [grant number 19K07849, to MS]; a grant from the Takeda Science Foundation to MS; and research grants from Pfizer Inc. [WS1878886], Nippon Zoki Pharmaceutical Co., Ltd, and Kao Corporation to our research group. This work was supported in part by a Japan-China Sasakawa Medical Fellowship [grant number 2017816] and a State Scholarship Fund of the China Scholarship Council [grant number 201908500072] to CT.

Declaration of Competing Interest

The authors declare that they have no conflict of interest.

Acknowledgements

We would like to thank Dr. Tsubasa Takizawa at Department of Neurology, Keio University School of Medicine, and Mr. Yasunao Ishida at Nippon Zoki Pharmaceutical Co., Ltd. for their advice and insightful discussions.

References

Ashina, M., Hansen, J.M., Do, T.P., Melo-Carrillo, A., Burstein, R., Moskowitz, M.A., 2019. Migraine and the trigeminovascular system-40 years and counting. Lancet Neurol. 18, 795–804.
Becerra, L., Bishop, J., Barmettler, G., Kainz, V., Burstein, R., Borsook, D., 2017. Brain network alterations in the inflammatory soup animal model of migraine. Brain Res. 1660, 36–46.
Blau, J.N., 1982. Resolution of migraine attacks: sleep and the recovery phase. J. Neurol. Neurosurg. Psychiatry 45, 223–226.
Bond, D.S., Thomas, J.G., O'Leary, K.C., Lipton, R.B., Peterlin, B.L., Roth, J., Rathier, L., Wing, R.R., 2015. Objectively measured physical activity in obese women with and without migraine. Cephalalgia 35, 886–893.
Borsook, D., Edwards, R., Elman, I., Becerra, L., Levine, J., 2013. Pain and analgesia: the value of salience circuits. Prog. Neurobiol. 104, 93–105.
Casili, G., Lanza, M., Filippone, A., Campolo, M., Paterniti, I., Cuzzocrea, S., Esposito, E., 2020. Dimethyl fumarate alleviates the nitroglycerin (NTG)-induced migraine in mice. J. Neuroinflammation 17, 59.
Charles, A.C., Baca, S.M., 2013. Cortical spreading depression and migraine. Nat. Rev. Neurol. 9, 637–644.

Chu, M.K., Im, H.J., Chung, C.S., Oh, K., 2011. Interictal pattern-induced visual discomfort and ictal photophobia in episodic migraineurs: an association of interictal and ictal photophobia. Headache 51, 1461–1467.
Danno, D., Kawabata, K., Tachibana, H., 2013. Three cases of nummular headache effectively treated with Neurotropin((R)). Intern. Med. 52, 493–495.
de Tommaso, M., Ambrosini, A., Brighina, F., Coppola, G., Perrotta, A., Pierelli, F., Sandrini, G., Valeriani, M., Marinazzo, D., Stramaglia, S., Schoenen, J., 2014. Altered processing of sensory stimuli in patients with migraine. Nat. Rev. Neurol. 10, 144–155.
Dodick, D.W., 2018a. Migraine. Lancet 391, 1315–1330.
Dodick, D.W., 2018b. A phase-by-Phase review of migraine pathophysiology. Headache 58 (Suppl 1), 4–16.
Ebine, T., Toriumi, H., Shimizu, T., Unekawa, M., Takizawa, T., Kayama, Y., Shibata, M., Suzuki, N., 2016. Alterations in the threshold of the potassium concentration to evoke cortical spreading depression during the natural estrous cycle in mice. Neurosci. Res. 112, 57–62.
Foster, S.A., Chen, C.C., Ding, Y., Mason, O., McGuiness, C.B., Morrow, P., Ye, W., Wade, R.L., Smith, T.R., Joshi, S., 2020. Economic burden and risk factors of migraine disease progression in the US: a retrospective analysis of a commercial payer database. J. Med. Econ. 23, 1356–1364.
Fukuda, Y., Berry, T.L., Nelson, M., Hunter, C.L., Fukuhara, K., Imai, H., Ito, S., Granholm-Bentley, A.C., Kaplan, A.P., Mutoh, T., 2010. Stimulated neuronal expression of brain-derived neurotrophic factor by Neurotropin. Mol. Cell. Neurosci. 45, 226–233.
Fukuda, Y., Fukui, T., Hikichi, C., Ishikawa, T., Murate, K., Adachi, T., Imai, H., Fukuhara, K., Ueda, A., Kaplan, A.P., Mutoh, T., 2015. Neurotropin promotes NGF signaling through interaction of GM1 ganglioside with Trk neurotrophin receptor in PC12 cells. Brain Res. 1596, 13–21.
Fukuda, Y., Nakajima, K., Mutoh, T., 2020. Neuroprotection by Neurotropin through crosstalk of neurotrophic and innate immune receptors in PC12 cells. Int. J. Mol. Sci., 21.
GBD 2016 Disease and Injury Incidence and Prevalence Collaborators, 2017. Global, regional, and national incidence, prevalence, and years lived with disability for 328 diseases and injuries for 195 countries, 1990-2016: a systematic analysis for the Global Burden of Disease Study 2016. Lancet 390, 1211–1259.
Giffin, N.J., Lipton, R.B., Silberstein, S.D., Olesen, J., Goadsby, P.J., 2016. The migraine postdrome: an electronic diary study. Neurology 87, 309–313.
Harriott, A.M., Chung, D.Y., Uner, A., Bozdayi, R.O., Morais, A., Takizawa, T., Qin, T., Ayata, C., 2021. Optogenetic spreading depression elicits trigeminal pain and anxiety behavior. Ann. Neurol. 89, 99–110.
Hata, T., Kita, T., Itoh, E., Oyama, R., Kawabata, A., 1988. Mechanism of the analgesic effect of neurotropin. Jpn. J. Pharmacol. 48, 165–173.
Headache Classification Committee of the International Headache Society, 2018. The international classification of headache disorders, 3rd edition. Cephalalgia 38, 1–211.
Iwashita, T., Shimizu, T., Shibata, M., Toriumi, H., Ebine, T., Funakubo, M., Suzuki, N., 2013. Activation of extracellular signal-regulated kinase in the trigeminal ganglion following both treatment of the dura mater with capsaicin and cortical spreading depression. Neurosci. Res. 77, 110–119.
Kato, S., Nakamura, H., Naiki, M., Takeoka, Y., Suehiro, S., 1991. Suppression of acute experimental allergic encephalomyelitis by neurotropin: clinical, histopathologic, immunologic and immunohistochemical studies. J. Neuroimmunol. 35, 237–245.
Kayama, Y., Shibata, M., Takizawa, T., Ibata, K., Shimizu, T., Ebine, T., Toriumi, H., Yuzaki, M., Suzuki, N., 2018. Functional interactions between transient receptor potential M8 and transient receptor potential V1 in the trigeminal system: relevance to migraine pathophysiology. Cephalalgia 38, 833–845.
Kelman, L., 2006. The postdrome of the acute migraine attack. Cephalalgia 26, 214–220.
Maleki, N., Becerra, L., Brawn, J., Bigal, M., Burstein, R., Borsook, D., 2012. Concurrent functional and structural cortical alterations in migraine. Cephalalgia 32, 607–620.
May, A., 2017. Understanding migraine as a cycling brain syndrome: reviewing the evidence from functional imaging. Neurol. Sci. 38, 125–130.
McAdams, H., Kaiser, E.A., Igdalova, A., Haggerty, E.B., Cucchiara, B., Brainard, D.H., Aguirre, G.K., 2020. Selective amplification of ipRGC signals accounts for interictal photophobia in migraine. Proc. Natl. Acad. Sci. U. S. A. 117, 17320–17329.
Mulleners, W.M., Aurora, S.K., Chronicle, E.P., Stewart, R., Gopal, S., Koehler, P.J., 2001. Self-reported photophobic symptoms in migraineurs and controls are reliable and predict diagnostic category accurately. Headache 41, 31–39.
Nakajo, Y., Yang, D., Takahashi, J.C., Zhao, Q., Kataoka, H., Yanamoto, H., 2015. ERV enhances spatial learning and prevents the development of infarcts, accompanied by upregulated BDNF in the cortex. Brain Res. 1610, 110–123.
Ng-Mak, D.S., Fitzgerald, K.A., Norquist, J.M., Banderas, B.F., Nelsen, L.M., Evans, C.J., Healy, C.G., Ho, T.W., Bigal, M., 2011. Key concepts of migraine postdrome: a qualitative study to develop a post-migraine questionnaire. Headache 51, 105–117.
Nishimoto, S., Okada, K., Tanaka, H., Okamoto, M., Fujisawa, H., Okada, T., Naiki, M., Murase, T., Yoshikawa, H., 2016. Neurotropin attenuates local inflammatory response and inhibits demyelination induced by chronic constriction injury of the mouse sciatic nerve. Biologicals 44, 206–211.
Noseda, R., Jakubowski, M., Kainz, V., Borsook, D., Burstein, R., 2011. Cortical projections of functionally identified thalamic trigeminovascular neurons: implications for migraine headache and its associated symptoms. J. Neurosci. 31, 14204–14217.
Okazaki, R., Namba, H., Yoshida, H., Okai, H., Miura, T., Kawamura, M., 2008. The antiallodynic effect of Neurotropin is mediated via activation of descending pain inhibitory systems in rats with spinal nerve ligation. Anesth. Analg. 107, 1064–1069.
Perenboom, M.J.L., Zamanipoor Najafabadi, A.H., Zielman, R., Carpay, J.A., Ferrari, M.D., 2018. Quantifying visual allodynia across migraine subtypes: the Leiden Visual Sensitivity Scale. Pain 159, 2375–2382.
Pietrobon, D., Moskowitz, M.A., 2014. Chaos and commotion in the wake of cortical spreading depression and spreading depolarizations. Nat. Rev. Neurosci. 15, 379–393.
Quintela, E., Castillo, J., Munoz, P., Pascual, J., 2006. Premonitory and resolution symptoms in migraine: a prospective study in 100 unselected patients. Cephalalgia 26, 1051–1060.
Rogers, D.G., Bond, D.S., Bentley, J.P., Smitherman, T.A., 2020. Objectively measured physical activity in migraine as a function of headache activity. Headache 60, 1930–1938.
Sakai, D., Nakai, T., Hiraishi, S., Nakamura, Y., Ando, K., Naiki, M., Watanabe, M., 2018. Upregulation of glycosaminoglycan synthesis by Neurotropin in nucleus pulposus cells via stimulation of chondroitin sulfate N-acetylgalactosaminyltransferase 1: a new approach to attenuation of intervertebral disc degeneration. PLoS One 13, e0202640.
Takeshima, T., Wan, Q., Zhang, Y., Komori, M., Stretton, S., Rajan, N., Treuer, T., Ueda, K., 2019. Prevalence, burden, and clinical management of migraine in China, Japan, and South Korea: a comprehensive review of the literature. J. Headache Pain 20, 111.
Tang, C., Unekawa, M., Kitagawa, S., Takizawa, T., Kayama, Y., Nakahara, J., Shibata, M., 2020. Cortical spreading depolarisation-induced facial hyperalgesia, photophobia and hypomotility are ameliorated by sumatriptan and olcegepant. Sci. Rep. 10, 11408.
Yoshii, H., Suehiro, S., Watanabe, K., Yanagihara, Y., 1987. Immunopharmacological actions of an extract isolated from inflamed skin of rabbits inoculated with vaccinia virus (neurotropin); enhancing effect on delayed type hypersensitivity response through the induction of Lyt-1+2- T cells. Int. J. Immunopharmacol. 9, 443–451.
Zhang, X., Levy, D., Noseda, R., Kainz, V., Jakubowski, M., Burstein, R., 2010. Activation of meningeal nociceptors by cortical spreading depression: implications for migraine with aura. J. Neurosci. 30, 8807–8814.
Zhang, X., Levy, D., Kainz, V., Noseda, R., Jakubowski, M., Burstein, R., 2011. Activation of central trigeminovascular neurons by cortical spreading depression. Ann. Neurol. 69, 855–865.
Zheng, Y., Fang, W., Fan, S., Liao, W., Xiong, Y., Liao, S., Li, Y., Xiao, S., Liu, J., 2018. Neurotropin inhibits neuroinflammation via suppressing NF-kappaB and MAPKs signaling pathways in lipopolysaccharide-stimulated BV2 cells. J. Pharmacol. Sci. 136, 242–248.